

Diamagnetic repulsion of particles for multilaminar flow assays†

Mark D. Tarn, Luke T. Elders, Sally A. Peyman‡ and Nicole Pamme*

We demonstrate diamagnetic repulsion forces for performing continuous multilaminar flow assays on particles based on their intrinsic properties and with a simple setup. The platform could be applied to sandwich assays on polystyrene particles, and to cell-based assays via their suspension in biologically benign magnetic media.

Functionalised microparticles are immensely popular for performing a variety of biochemical procedures,¹ and as such have been employed extensively in microfluidics² for a range of processes including separations,³⁻⁵ biosensing⁶ and immunoassays.⁷⁻⁹ On-chip immunoassays in particular have benefitted from their small size, high surface-to-volume ratio, and the ability to manipulate them within the well-defined and well-controlled environment of microfluidic structures. Often, such assays are performed by trapping functionalised particles within a microchannel, before consecutively flushing reagent and washing over the particle plug or individual particles and monitoring the response. However, this requires multiple steps that result in time-consuming processes and the use of relatively large volumes of reagents, and either the manual changing of solutions or the incorporation of more complex valving technologies.

In recent years, multilaminar flow reactions and assays have become very popular methods of performing particle-based reactions.¹⁰ Here, multiple laminar streams of alternating reagent and washing buffer solutions are generated across a microfluidic chamber, through which functionalised microparticles are deflected in order to perform reactions. A number of forces can be applied in order to manipulate the particles across the chamber, including

acoustic,¹¹⁻¹³ optical,¹⁴ dielectrophoretic,¹⁵ and inertial forces,¹⁶ biomolecular motors,^{17, 18} pinched flow,¹⁹ hydrodynamic filtration,²⁰ and physical objects.²¹⁻²³ Magnetic forces^{6, 24-28} have arguably been the most successful particle manipulation method in multilaminar flow systems, with functionalised magnetic particles being deflected across laminar reagent streams via permanent magnets for applications including assays,²⁹⁻³⁵ DNA hybridisation,^{36, 37} DNA extraction,^{38, 39} oligonucleotide capture,^{40, 41} and particle coating.⁴²⁻⁴⁵ However, while magnetic forces provide simplicity and excellent control they require the use of magnetic microparticles,^{24, 25} which can be very expensive, or the labelling of cells with a magnetic tag.^{25, 28} An alternative approach would be to employ the use of diamagnetic repulsion forces, which have thus far not been demonstrated for multilaminar flow reaction processes.

Diamagnetism is an intrinsic property of all materials, but is masked by any other magnetic properties that the material may have (e.g. ferromagnetism, paramagnetism). Materials that only exhibit diamagnetic properties have a magnetic susceptibility (χ) less than zero, as opposed to the other types of magnetism where χ is greater than zero. For example, nearly all biological cells are diamagnetic, as are most polymers unless specifically manufactured to be otherwise, and so they are each susceptible to repulsion from magnetic fields. However, the repulsion forces are actually very weak, and so are typically not encountered in normal conditions. The magnetic forces (F_{mag}) applied to a material, in this case a microparticle, are dependent on a number of factors, as shown in Equation (1):

$$F_{\text{mag}} = \frac{(\chi_p - \chi_m) V (\mathbf{B} \cdot \nabla) \mathbf{B}}{\mu_0} \quad (1)$$

Department of Chemistry, University of Hull, Cottingham Road, Hull, HU6 7RX, UK.
* E-mail: n.pamme@hull.ac.uk; Tel: +44 (0) 1482 465027; Fax: +44 (0) 466410.

† Electronic Supplementary Information (ESI) available: Photographs showing the effect of biotin-4-fluorescein on ferrofluid stability, images of laminar flow in the the 10-inlet/9-outlet microfluidic device, magnetic field simulations, and a concept for an optimised multilaminar flow reaction platform. See DOI: 10.1039/x0xx00000x

‡ Current address: School of Physics and Astronomy, University of Leeds, Woodhouse Lane, Leeds, LS2 9JT, UK.

χ_p is the magnetic susceptibility of a microparticle, χ_m is the magnetic susceptibility of the medium that the microparticle is suspended within, V is the volume of the microparticle, \mathbf{B} is the magnetic flux density of the magnetic field, and μ_0 is the permeability of free space ($4\pi \times 10^{-7} \text{ H m}^{-1}$). The equation shows how, when a diamagnetic particle ($\chi_p < 0$) is suspended

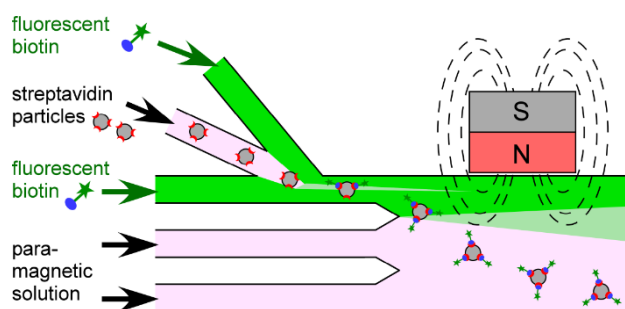


Fig. 1 Principle of multilaminar flow-based reactions via diamagnetic repulsion of particles. Here, laminar flow streams of paramagnetic washing solution and fluorescently labelled biotin (also in paramagnetic solution) are generated across a

microfluidic chamber. Streptavidin-functionalised polymer particles suspended in paramagnetic solution are introduced into a flow focusing region of the chip, whereupon they are repelled by a permanent magnet through the biotin reagent stream and into a washing stream, enabling a one-step multilaminar flow reaction with detection achieved via fluorescence. Biotin diffusion is shown as a light green cone.

in a magnetic medium ($\chi_m > 0$), the difference in magnetic susceptibility ($\chi_p - \chi_m$) is negative, resulting in a negative F_{mag} force that indicates repulsion from the magnetic field. Suspending a diamagnetic particle in a magnetic medium is most easily achieved via two methods: (i) an aqueous solution of dissolved paramagnetic ions (e.g. Mn^{2+} or Gd^{3+}),⁴⁶⁻⁴⁸ and (ii) using an aqueous-based ferrofluid consisting of a colloidal suspension of iron oxide nanoparticles.^{49, 50}

The ability to combine the benefits of magnetic forces with the manipulation of diamagnetic materials based on their intrinsic properties has, in recent years, resulted in some use of diamagnetic repulsion as a label free manipulation force in microfluidic platforms. The small dimensions of the channels, and the close proximity that can be attained between the permanent magnets to the channels, means that diamagnetic particles and cells can easily be handled within microfluidic devices. Applications that have been demonstrated using this technique have included the trapping,^{47, 48, 51-58} focussing,^{47, 59-62} and deflection^{47, 63-73} of particles, cells, and droplets. Continuous flow processes have been performed using on-chip diamagnetic repulsion, but have largely consisted particle and cell separations in paramagnetic solutions^{46, 64, 69-71, 74} and ferrofluids.^{66, 73, 75-78} Previously, we have demonstrated how immunoassays could be performed on functionalised polymer particles that have been trapped as a plug in paramagnetic solution in a microchannel.^{44, 47}

Here, for the first time, we investigate the potential of diamagnetic repulsion for performing multilaminar flow-based reactions in both paramagnetic solutions and ferrofluid. Fig. 1 demonstrates the basic principle of the multilaminar flow

the technique. Streams of magnetic washing solution and fluorescently labelled biotin in magnetic solution are generated across a microfluidic chamber via a flow focusing channel, into which streptavidin-functionalised polymer particles, also suspended in magnetic solution are introduced. As the particles traverse the chamber, they are deflected laterally via repulsion from a permanent magnet, thereby passing through the biotin reagent stream and into the washing stream where the success of the reaction can be determined via fluorescence.

Firstly, the ability to perform simple bioassays was assessed by attempting the streptavidin-biotin binding reaction in both types of magnetic media: paramagnetic solution and ferrofluid. 10 μm diameter polystyrene particles

($\chi_p = -8.21 \times 10^{-6}$, $\rho = 1050 \text{ kg m}^{-3}$) functionalised with streptavidin groups (Micromer Streptavidin) were purchased from Micromod Partikeltechnologie (Germany), while fluorescently labelled biotin (biotin-4-fluorescein, $\lambda_{em} = 494 \text{ nm}$, $\lambda_{ex} = 521 \text{ nm}$) was purchased from Molecular Probes (Life Technologies, UK). An aqueous paramagnetic solution of 0.79 M manganese(II) chloride (Sigma-Aldrich, UK) was prepared,

giving a 10 % w/v $MnCl_2$ ($\chi_m = 1.46 \times 10^{-4}$, $\eta = 1.31 \times 10^{-3} \text{ kg m}^{-1} \text{ s}^{-1}$, $\rho = 1083 \text{ kg m}^{-3}$ at 20 °C) that had previously yielded optimum diamagnetic repulsion behaviour in our microfluidic devices.^{47, 63} The solution also contained 0.01 % w/v Tween20

surfactant (Sigma-Aldrich) in order to prevent particles sticking. Aqueous-based ferrofluid (EMG 507) was purchased from Ferrotec (USA) and diluted 0.01x in purified water with the addition of 0.01 % w/v Tween20. A 0.01x dilution of ferrofluid has been shown to give suitable diamagnetic repulsion responses in microfluidic devices while allowing visualisation of particles and cells.^{66, 75, 78}

6.5 μL of stock streptavidin particle suspension (4.6×10^7 particles mL^{-1}) was diluted in 1000 μL of 0.79 M $MnCl_2$ to a final concentration of approximately 3×10^5 particles mL^{-1} . Separately, a solution of biotin-4-fluorescein was dissolved in 0.79 M $MnCl_2$ to a concentration of 1 $\mu g \text{ mL}^{-1}$ (1.55 μM). 200

process in paramagnetic solution, in which a streptavidin-

μL of the particle suspension was added to 200 μL of the fluorescently labelled biotin solution in an Eppendorf tube (1.5 mL, VWR, UK) and mixed on a vortexer, then allowed to incubate for 20 min on a rotator. Eppendorf tubes containing the fluorescently labelled biotin were wrapped in aluminium foil to protect them from light. The particles were then collected as a plug by centrifuging for 5 min at 5000 rpm, and the supernatant removed. The particles were washed by

biotin binding reaction is performed as a proof-of-concept of

re-suspending them in MnCl_2 solution, vortexing the tube, and performing centrifugation again. This washing process was repeated twice more in MnCl_2 , then a portion of the solution added to a microscope slide and viewed under an inverted fluorescence microscope (TE-2000, Nikon, UK). The particles clearly showed an increase in their fluorescence intensity compared to unreacted particles, indicating that the streptavidin-biotin assay was successful, and thus a viable option for multilaminar flow studies. This also reiterated previous results in which assays were performed in MnCl_2 .^{47, 51}

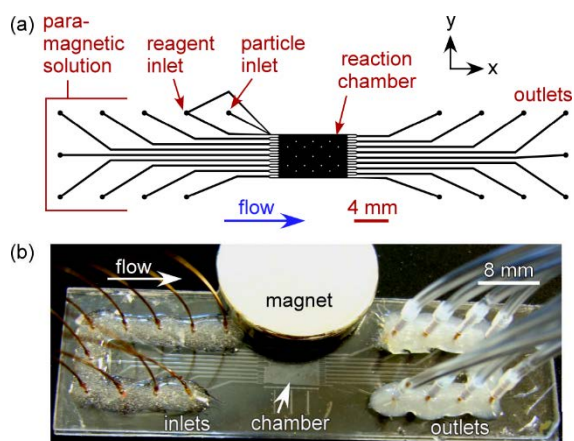


Fig. 2 (a) CAD design of the microfluidic device, featuring a reaction chamber fed by 10 inlet channels, including a flow focussing section for the introduction of reagents and functionalised polymer particles, and with 9 outlet channels. (b) Photograph of the glass device with interfaced tubing and a 20 mm \varnothing x 5 mm NdFeB magnet placed on the chip, next to the chamber.

Attempts were made to repeat the above process in 0.01x diluted EMG 507 ferrofluid, but upon attempting to dissolve the biotin-4-fluorescein in the solution the ferrofluid began to form clumps that settled to the bottom of the vial after several minutes. Clearly, the presence of the fluorescently labelled biotin caused the magnetic nanoparticles, which in this case were stabilised by anionic surfactant, to agglomerate and drop out of suspension, and this effect is shown in Fig. S1 in the ESI. Therefore, despite its potential for offering greater diamagnetic repulsion forces, the aqueous ferrofluid was clearly unsuitable for performing multilaminar flow reactions, at least for this particular reagent. Therefore, based on the off-chip tests in MnCl_2 and ferrofluid, subsequent on-chip experiments were performed in paramagnetic 0.79 M MnCl_2 solution.

The microfluidic device employed for these multilaminar flow tests was fabricated in B270 glass (Telic, CA, USA) to a depth of 20 μm using standard photolithography and wet etching techniques.⁷⁹ The chip design is shown in Fig. 2a. It featured an 8 mm x 5.2 mm reaction chamber supported by 17 square posts (200 μm x 200 μm each), with a total of 10 inlet channels including the flow focussing structure. This flow focussing part consisted of two reagent (fluorescently labelled biotin) inlet channels fed by a single access hole, which diverged around a single particle inlet channel. These channels were 240 μm wide at the access hole, then tapered to a width of 120 μm at the chamber entrance. The remaining 8 inlet channels, used for the introduction of 0.79 M MnCl_2 washing

solution, each had an initial width of 240 μm wide, before splitting into parallel channels of 120 μm width at the chamber entrance. The outlet system also consisted of 9 outlet channels which (240 μm width), 8 of which split into parallel channels (120 μm width) at the exit of the chamber, with the remaining channel tapering to 120 μm width at the chamber. 400 μm diameter access holes were drilled into the glass plate, and the etched plate thermally bonded with a glass top plate. This chip design was not originally envisaged for this type of experiment, hence the large number of MnCl_2 washing channels, but it was adapted for the purpose since it featured the flow focussing region that would allow narrow streams of reagent to be introduced alongside a suspension of particles.

The chip was interfaced to a syringe pump (Pump PHD 22/2000 with a 10-syringe rack, Harvard Apparatus, UK) and to a waste vial as described previously.³⁰ Briefly, fused silica capillaries (150 μm ID, 363 μm OD, CM Scientific, UK) were glued into the access holes of the chip using Araldite Rapid epoxy resin (RS Components, UK). The outlet capillaries were connected to a waste vial using a combination of PTFE tubing (0.3 mm ID, 1.8 mm OD, Sigma-Aldrich, UK) and Tygon tubing (1 mm ID, 1.8 mm OD, Cole-Parmer, UK). The chip was placed on the inverted fluorescence microscope (Nikon) fitted with a CCD camera (Retiga-EXL), with Image-Pro Plus 6 software used to capture images. Images were then analysed using ImageJ software (<http://imagej.nih.gov/ij/>).

The laminar flow regime of the microfluidic device was first tested by introducing alternating streams of red and yellow printer ink into the chip (see Fig. S2 in the ESI). The flow streams in the reaction chamber near the bottom of the image were diverted slightly from a linear path due to higher flow resistances in the longer middle channels. This caused flow to be directed towards the shorter exit channels near to the edge of the chip. However, the laminar flow streams in the region of the chamber where the particles and reagent stream would be introduced (near the top of the image) were sufficiently stable.

The on-chip streptavidin-biotin assay was carried out by placing a cylindrical 20 mm \varnothing x 5 mm neodymium-iron-boron (NdFeB) magnet (Magnet Sales, UK) on top of the glass chip, next to the reaction chamber (Fig. 2b). The magnetic field generated across the chamber was simulated using Finite Element Method Magnetics (FEMM 4.2) software, based on a magnetic flux density (\mathbf{B}) at the magnet surface that had been calculated to be approximately 275 mT. The resulting simulations are shown in Fig. S3 in the ESI. From these, the average value of \mathbf{B} in the region of the chamber where the particles would be present was 307 mT, with a gradient ($\nabla\mathbf{B}$) of 48 mT mm^{-1} , yielding a $(\mathbf{B}\cdot\nabla)\mathbf{B}$ value of 14.7 T^2m^{-1} . However, given that FEMM is a two-dimensional modelling software, these values were only an estimate since the cylindrical shape of the magnet could not be accounted for.

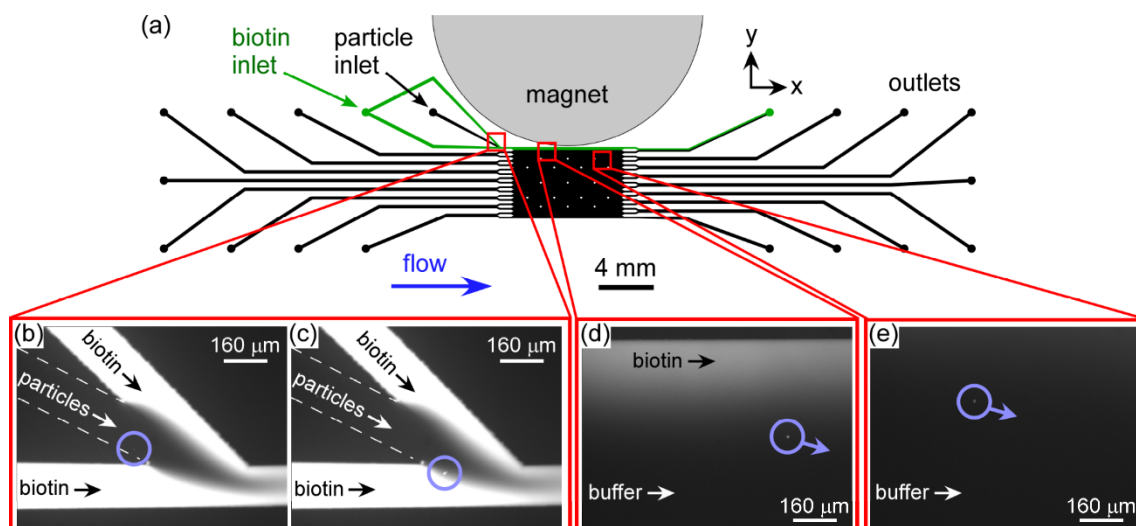


Fig. 3 (a) Schematic of the device and setup used for the diamagnetic repulsion-based streptavidin-biotin assay. All solutions contained paramagnetic MnCl_2 solution. (b) A streptavidin-functionalised polymer particle (highlighted) immediately prior to entering a stream of fluorescently labelled biotin. The repulsion effect forced the diamagnetic particles against the side wall of the inlet channel. (c) The same particle as it entered the fluorescently labelled biotin reagent stream, immediately showing an increase in fluorescence intensity. (d) Deflection of a reacted particle out of the biotin stream and into a washing stream. (e) Particle having fully exited the reagent stream, allowing its analysis by fluorescence.

The chip was flushed consecutively with ethanol, water, and 0.79 MnCl_2 solution. Next, a 250 μL glass syringe (SGE, Sigma-Aldrich, UK) was filled with streptavidin-functionalised particle suspension (3×10^5 particles mL^{-1}) and connected to the particle inlet, while a 100 μL glass syringe (SGE) was filled with a solution of biotin-4-fluorescein ($10 \mu\text{g mL}^{-1}$) in 0.79 M

MnCl_2 and connected to the reagent inlet. Eight 1 mL plastic syringes (BD Plastipak) were filled with 0.79 M MnCl_2 washing solution (Fig. 2a) and connected to the remaining inlet capillaries. A flow rate of $1 \mu\text{L h}^{-1}$ was applied via the syringe pump, relative to the 1 mL syringes containing washing solution. Since the 100 μL (biotin reagent) and 250 μL (particle suspension) glass syringes, having smaller inner diameters,

were on the same syringe pump as the 1 mL syringes (at $1 \mu\text{L h}^{-1}$), this yielded flow rates of $0.33 \mu\text{L h}^{-1}$ and $0.52 \mu\text{L h}^{-1}$ for the biotin and particle suspension, respectively.

The relatively low flow rate of the biotin-4-fluorescein reagent solution compared to the particle input rate and the MnCl_2 washing solution allowed a narrow stream of solution to

be generated. Furthermore, by applying a higher flow rate of the washing solution, the biotin stream was forced in the y -direction towards the side wall of the chamber, towards the magnet, thus attempting to constrain the stream against the wall. These were important actions since the diamagnetic repulsion forces (F_{mag}) on the particles would be small, estimated to be ~ 1 pN using Equation 1, based on the particle and media properties and the magnetic field simulations (Fig S3 in the ESI). Therefore, the shorter the distance (in the y -direction) that the particles were required to travel to traverse the reagent stream the better. This was particularly important since at such low flow rates the diffusion of biotin reagent becomes greater, hence the stream was constricted against the wall to try to limit the diffusion distance of the biotin across the chamber, and to reduce the distance over which a particle must travel to reach the washing stream. As the streptavidin-functionalised particles entered the flow focussing region (Fig. 3), they were pushed towards the lower edge (in the y -direction) of the particle inlet channel via repulsion from the magnet (Fig. 3b), entering the reagent stream and immediately exhibiting an increase in fluorescence intensity (Fig. 3c) as the biotin-4-fluorescein became bound to the streptavidin groups on the particle surfaces. As they then entered the chamber they were further deflected in the y -direction, away from the magnet and out of the biotin stream (Fig. 3d). The particle

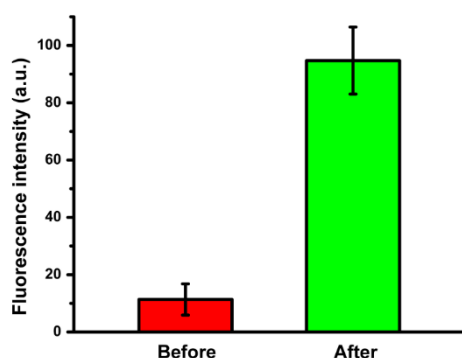


Fig. 4 Fluorescence intensities of the streptavidin-functionalised polystyrene particles before and after passing through the biotin-4-fluorescein reagent stream, demonstrating a clear increase in intensity that indicates successful binding events ($n = 13$).

trajectories were similar to those that had been observed in previous experiments under similar conditions.⁴⁷

The particles continued to be repelled from the magnet as they passed through the chamber, until they had fully entered the MnCl₂ washing streams, where any unbound reagent was washed from the particle surface (Fig. 3e). The fluorescence intensities of the particles were measured in this washing stream and compared to the intensities prior to entering the biotin-4-fluorescein stream, and these are shown in Fig. 4. The polystyrene particles exhibit a degree of autofluorescence, hence the non-zero intensity on the plot prior to the reaction. The results show a clear increase in fluorescence after crossing the reagent stream into the washing stream, indicating successful binding of the biotin to the streptavidin-coated particles.

Thus, we have demonstrated a proof-of-principle streptavidin-biotin assay via diamagnetic repulsion. This initial work represents a first step towards the development of a more bespoke diamagnetic multiflow reaction platform that would incorporate a number of features to optimise and improve the system. One concern of such a platform is the diffusion of the reagent at the low flow rates currently employed due to the weak magnetic forces employed: in order for this system to be viable for performing immunoassays or other reactions, it must be possible to deflect the particles further than the reagent can diffuse to ensure complete washing. For example, based on a biotin-4-fluorescein hydrodynamic radius of 0.63 nm (determined from its diffusion coefficient in water^{29, 80}), which would yield a diffusion

coefficient of $2.6 \times 10^{-10} \text{ m}^2 \text{ s}^{-1}$ in the 0.79 M MnCl₂ medium at

the applied flow rate, we calculated the diffusion distance of the reagent to be 419 μm in the y-direction as it flowed through the chamber. On the other hand, the magnetically induced velocity of the diamagnetic particles (estimated as being $4.3 \mu\text{m s}^{-1}$)^{63, 81} would result in a deflection distance of 1794 μm ; much greater than the extent of reagent diffusion and so ensuring that the particles would fully enter the washing stream. Bearing in mind that most biomolecules used in processes such as immunoassays are much larger than the reagent used here, the effect of diffusion would therefore be less in such systems. While the current system is clearly suitable for one-step reactions, performing a two-step reaction with the requisite extra reagent and washing streams would require further optimisation and enhancement of the particle repulsion in order to deflect them through multiple streams.

Conclusions

We have demonstrated a proof-of-principle binding assay for performing multilaminar flow assays and reactions on particles based on their intrinsic properties by diamagnetic repulsion, simply by using an inexpensive permanent magnet and a paramagnetic medium. These initial experiments demonstrate the potential of the technique for deflecting particles through multiple laminar streams of reagents and washing solutions, though the migration distances achieved here limited the technique to only one reaction step. However, this could be

greatly improved and optimised by employing more paramagnetic solutions, such as those containing Gd³⁺ salts that have a higher magnetic susceptibility than Mn²⁺ salts.^{46, 54, 59, 74} While ferrofluid was found to be unsuitable for preparation of the reagent solution here, different types of reagents may be more amenable to being dissolved in ferrofluid without destabilising the colloidal system of magnetic nanoparticles, thereby enabling much greater repulsion forces.

The magnetic field could be more finely tuned, for example by incorporation of magnetisable microstructures into the chip, which has been used to great effect for the diamagnetic separation of live cells.⁷⁴ These improvements could allow much greater F_{mag} forces that would be employed with a view to multi-step reactions such as sandwich immunoassays, the concept of which is shown in Fig. S4 in the ESI. Furthermore, reactions and assays on living cells could also be achieved by using paramagnetic media prepared from gadolinium(III) diethylenetriaminepentaacetic acid (Gd-DTPA), a magnetic resonance imaging (MRI) contrast agent that has been shown to allow diamagnetic repulsion of cells while maintaining their viability.^{54, 59, 74} With this in mind, further investigation of this technique could lead to a simple but powerful method for particle and cell based reactions with minimal apparatus required.

References

1. H. Kawaguchi, *Prog. Polym. Sci.*, 2000, **25**, 1171-1210.
2. M. D. Tarn and N. Pamme, in *Elsevier Reference Module in Chemistry, Molecular Sciences and Chemical Engineering*, ed. J. Reedijk, Elsevier, Waltham, MA, 2013.
3. N. Pamme, *Lab Chip*, 2007, **7**, 1644-1659.
4. A. Lenshof and T. Laurell, *Chem. Soc. Rev.*, 2010, **39**, 1203-1217.
5. P. Sajeesh and A. Sen, *Microfluid. Nanofluid.*, 2014, **17**, 1-52.
6. A. van Reenen, A. M. de Jong, J. M. J. den Toonder and M. W. J. Prins, *Lab Chip*, 2014, **14**, 1966-1986.
7. M. D. Tarn and N. Pamme, *Expert Rev. Mol. Diagn.*, 2011, **11**, 711-720.
8. C. T. Lim and Y. Zhang, *Biosens. Bioelectron.*, 2007, **22**, 1197-1204.
9. A. H. C. Ng, U. Uddayasankar and A. R. Wheeler, *Anal. Bioanal. Chem.*, 2010, **397**, 991-1007.
10. M. D. Tarn, M. J. Lopez-Martinez and N. Pamme, *Anal. Bioanal. Chem.*, 2014, **406**, 139-161.
11. P. Augustsson, J. Malm and S. Ekstrom, *Biomicrofluidics*, 2012, **6**, 034115.
12. S. Li, X. Ding, Z. Mao, Y. Chen, N. Nama, F. Guo, P. Li, L. Wang, C. E. Cameron and T. J. Huang, *Lab Chip*, 2015, **15**, 331-338.
13. G. Destgeer, B. H. Ha, J. Park, J. H. Jung, A. Alazzam and H. J. Sung, *Anal. Chem.*, 2015, **87**, 4627-4632.
14. T. Wang, S. Oehrlein, M. M. Somoza, J. R. Sanchez Perez, R. Kershner and F. Cerrina, *Lab Chip*, 2011, **11**, 1629-1637.

15. R. Tornay, T. Braschler, N. Demierre, B. Steitz, A. Finka, H. Hofmann, J. A. Hubbell and P. Renaud, *Lab Chip*, 2008, **8**, 267-273.
16. J. S. Dudani, D. E. Go, D. R. Gossett, A. P. Tan and D. Di Carlo, *Anal. Chem.*, 2014, **86**, 1502-1510.
17. T. Kim, L.-J. Cheng, M.-T. Kao, E. F. Hasselbrink, L. Guo and E. Meyhofer, *Lab Chip*, 2009, **9**, 1282-1285.
18. D. Steuerwald, S. M. Fruh, R. Griss, R. D. Lovchik and V. Vogel, *Lab Chip*, 2014, **14**, 3729-3738.
19. Y.-Y. Chiang and J. West, *Lab Chip*, 2013, **13**, 1031-1034.
20. S. Yang, A. Undar and J. D. Zahn, *Lab Chip*, 2007, **7**, 588-595.
21. K. J. Morton, K. Loutherbach, D. W. Inglis, O. K. Tsui, J. C. Sturm, S. Y. Chou and R. H. Austin, *Lab Chip*, 2008, **8**, 1448-1453.
22. C. Kantak, S. Beyer, L. Yobas, T. Bansal and D. Trau, *Lab Chip*, 2011, **11**, 1030-1035.
23. R. D. Sochol, S. Li, L. P. Lee and L. Lin, *Lab Chip*, 2012, **12**, 4168-4177.
24. N. Pamme, *Lab Chip*, 2006, **6**, 24-38.
25. N. Pamme, *Curr. Opin. Chem. Biol.*, 2012, **16**, 436-443.
26. M. A. M. Gijs, *Microfluid. Nanofluid.*, 2004, **1**, 22-40.
27. M. A. M. Gijs, F. Lacharme and U. Lehmann, *Chem. Rev.*, 2010, **110**, 1518-1563.
28. M. Hejazian, W. Li and N.-T. Nguyen, *Lab Chip*, 2015, **15**, 959-970.
29. S. A. Peyman, A. Iles and N. Pamme, *Chem. Commun.*, 2008, 1220-1222.
30. S. A. Peyman, A. Iles and N. Pamme, *Lab Chip*, 2009, **9**, 3110-3117.
31. L. Sasso, I. Johnston, M. Zheng, R. Gupte, A. Ündar and J. Zahn, *Microfluid. Nanofluid.*, 2012, **13**, 603-612.
32. L. A. Sasso, K. Aran, Y. Guan, A. Ündar and J. D. Zahn, *Artif. Organs.*, 2013, **37**, E9-E17.
33. L. A. Sasso, A. Undar and J. D. Zahn, *Microfluid. Nanofluid.*, 2010, **9**, 253-265.
34. F. Ibraimi, D. Kriz, M. Lu, L. O. Hansson and K. Kriz, *Anal. Bioanal. Chem.*, 2006, **384**, 651-657.
35. Y. Gao, A. W. Y. Lam and W. C. W. Chan, *ACS Appl. Mater. Interfaces*, 2013, **5**, 2853-2860.
36. S. A. Peyman, H. Patel, N. Belli, A. Iles and N. Pamme, *Magneto-hydrodynamics*, 2009, **45**, 361-370.
37. M. Vojtišek, A. Iles and N. Pamme, *Biosens. Bioelectron.*, 2010, **25**, 2172-2176.
38. M. Karle, J. Miwa, G. Czilwik, V. Auwaerter, G. Roth, R. Zengerle and F. von Stetten, *Lab Chip*, 2010, **10**, 3284-3290.
39. M. Karle, J. Woehrle, J. Miwa, N. Paust, G. Roth, R. Zengerle and F. von Stetten, *Microfluid. Nanofluid.*, 2011, **10**, 935-939.
40. R. Ganguly, T. Hahn and S. Hardt, *Microfluid. Nanofluid.*, 2010, **8**, 739-753.
41. T. Baier, S. Mohanty, K. S. Drese, F. Rampf, J. Kim and F. Schoenfeld, *Microfluid. Nanofluid.*, 2009, **7**, 205-216.
42. M. D. Tarn, R. F. Fakhruddin, V. N. Paunov and N. Pamme, *Mater. Lett.*, 2013, **95**, 182-185.
43. B.-U. Moon, N. Hakimi, D. K. Hwang and S. S. H. Tsai, *Biomicrofluidics*, 2014, **8**, 052103.
44. S. S. H. Tsai, J. S. Wexler, J. Wan and H. A. Stone, *Appl. Phys. Lett.*, 2011, **99**, 153509.
45. S. S. H. Tsai, J. S. Wexler, J. Wan and H. A. Stone, *Lab Chip*, 2013, **13**, 119-125.
46. A. Winkleman, R. Perez-Castillejos, K. L. Gudiksen, S. T. Phillips, M. Prentiss and G. M. Whitesides, *Anal. Chem.*, 2007, **79**, 6542-6550.
47. S. A. Peyman, E. Y. Kwan, O. Margaron, A. Iles and N. Pamme, *J. Chromatogr. A*, 2009, **1216**, 9055-9062.
48. H. Watarai and M. Namba, *Anal. Sci.*, 2001, **17**, 1233.
49. M. Hejazian and N.-T. Nguyen, *Lab Chip*, 2015, **15**, 2998-3005.
50. N.-T. Nguyen, *Microfluid. Nanofluid.*, 2012, **12**, 1-16.
51. M. D. Tarn, S. A. Peyman and N. Pamme, *RSC Adv.*, 2013, **3**, 7209-7214.
52. J. J. Wilbanks, G. Kiessling, J. Zeng, C. Zhang, T.-R. Tzeng and X. Xuan, *J. Appl. Phys.*, 2014, **115**, 044907.
53. J. Zeng, C. Chen, P. Vedantam, T.-R. Tzeng and X. Xuan, *Microfluid. Nanofluid.*, 2013, **15**, 49-55.
54. A. Winkleman, K. L. Gudiksen, D. Ryan, G. M. Whitesides, D. Greenfield and M. Prentiss, *Appl. Phys. Lett.*, 2004, **85**, 2411.
55. H. Watarai and M. Namba, *Anal. Sci.*, 2001, **17**, i169-i171.
56. H. Watarai and M. Namba, *J. Chromatogr. A*, 2002, **961**, 3-8.
57. T. Kimura, Y. Sato, F. Kimura, M. Iwasaka and S. Ueno, *Langmuir*, 2005, **21**, 830-832.
58. H. Chetouani, C. Jeandey, V. Haguët, H. Rostaing, C. Dieppedale and G. Reyne, *IEEE Trans. Magn.*, 2006, **42**, 3557-3559.
59. A. I. Rodriguez-Villarreal, M. D. Tarn, L. A. Madden, J. B. Lutz, J. Greenman, J. Samitier and N. Pamme, *Lab Chip*, 2011, **11**, 1240-1248.
60. T. Zhu, R. Cheng and L. Mao, *Microfluid. Nanofluid.*, 2011, **11**, 695-701.
61. L. Liang and X. Xuan, *Microfluid. Nanofluid.*, 2012, **13**, 637-643.
62. J. Zeng, C. Chen, V. Pallavi, V. Brown, T.-R. J. Tzeng and X. Xuan, *J. Micromech. Microeng.*, 2012, **22**, 105018.
63. M. D. Tarn, N. Hirota, A. Iles and N. Pamme, *Sci. Technol. Adv. Mater.*, 2009, **10**, 014611.
64. M. Vojtišek, M. D. Tarn, N. Hirota and N. Pamme, *Microfluid. Nanofluid.*, 2012, **13**, 625-635.
65. T. Zhu, D. Lichlyter, M. Haidekker and L. Mao, *Microfluid. Nanofluid.*, 2011, **10**, 1233-1245.
66. L. Liang, C. Zhang and X. Xuan, *Appl. Phys. Lett.*, 2013, **102**, 234101.
67. J. Zhu, L. Liang and X. Xuan, *Microfluid. Nanofluid.*, 2012, **12**, 65-73.
68. L. Liang, J. Zhu and X. Xuan, *Biomicrofluidics*, 2011, **5**, 034110.
69. Y. K. Hahn and J. K. Park, *Lab Chip*, 2011, **11**, 2045-2048.
70. J. H. Kang, S. Choi, W. Lee and J. K. Park, *J. Am. Chem. Soc.*, 2008, **130**, 396-397.
71. M. Kawano and H. Watarai, *Anal. Bioanal. Chem.*, 2012, **403**, 2645-2653.

72. K. Zhang, Q. Liang, X. Ai, P. Hu, Y. Wang and G. Luo, *Lab Chip*, 2011, **11**, 1271-1275.
73. T. Zhu, R. Cheng, Y. Liu, J. He and L. Mao, *Microfluid. Nanofluid.*, 2014, **17**, 973-982.
74. F. Shen, H. Hwang, Y. K. Hahn and J.-K. Park, *Anal. Chem.*, 2012, **84**, 3075-3081.
75. J. Zeng, Y. Deng, P. Vedantam, T.-R. Tzeng and X. Xuan, *J. Magn. Magn. Mater.*, 2013, **346**, 118-123.
76. T. Zhu, F. Marrero and L. Mao, *Microfluid. Nanofluid.*, 2010, **9**, 1003-1009.
77. T. Zhu, R. Cheng, S. Lee, E. Rajaraman, M. Eiteman, T. Querec, E. Unger and L. Mao, *Microfluid. Nanofluid.*, 2012, **13**, 645-654.
78. L. Liang and X. Xuan, *Biomicrofluidics*, 2012, **6**, 044106.
79. T. McCreedy, *Anal. Chim. Acta*, 2001, **427**, 39-43.
80. A. E. Kamholz, E. A. Schilling and P. Yager, *Biophys. J.*, 2001, **80**, 1967-1972.
81. Y. Iiguni, M. Suwa and H. Watarai, *J. Chromatogr. A*, 2004, **1032**, 165-171.